JOURNAL OF PROPULSION AND POWER
Vol. 15, No. 1, January–February 1999

Critical Assessment of Dual-Bell Nozzles

Manuel Frey* and Gerald Hagemann†
DLR, German Aerospace Research Center, 74239, Lampoldshausen, Germany

A critical assessment of dual-bell nozzles is given in this paper. The principal flowfield development in dual-bell nozzles, as well as design aspects for the contour of the base nozzle, the wall inflection, and the nozzle extension are discussed. Special regard is focused on the transition behavior from sea level to altitude operation and its dependence on the contour type used for the nozzle extension. Parametric numerical simulations of the flowfield development were performed to quantify the different loss effects. It is shown that the additional performance losses caused by the dual-bell nozzle contour are surprisingly low. An analytical derivation of the flow transients from the separated to the fully attached flow is presented. The necessity of further experimental investigations on dual-bell nozzles is emphasized, which will lead to a better understanding of the flow transition in dual-bell nozzles. Finally, new ideas are presented to minimize the duration of the critical flow transition by varying the thrust chamber pressure on system level, to ensure a sudden and controlled jump of the separation point from the wall inflection (sea-level operation) to the exit plane (altitude operation).

Nomenclature

A	= area
g	= gravity constant
h	= flight altitude
I_{sp}	= specific impulse
M	= Mach number
$\dot{m}$	= mass flow rate
p	= pressure
R	= specific gas constant
r_t	= throat radius
T	= temperature
t, T_{tr}	= time
v, w	= velocity
x, y, z	= Cartesian coordinates
β	= nozzle exit angle
γ	= contour inflection angle
δ	= scattering of separation criterion
ε	= nozzle area ratio
Π	= relative pressure difference

Subscripts

a	= ambient
B	= base nozzle
c	= combustion chamber
E	= nozzle extension
e	= exit plane
l	= lower
ref	= reference
rel	= relative
sl	= sea level
tr	= transition
u	= upper
vac	= vacuum
w	= wall

Presented as Paper 97-3299 at the AIAA/ASME/SAE/ASEE 33rd Joint Propulsion Conference, Seattle, WA, July 6–9, 1997; received Aug. 20, 1997; revision received June 13, 1998; accepted for publication June 18, 1998.

*Research Engineer, Ph.D. Candidate. E-mail: manuel.frey@dlr.de.
†Research Engineer, Ph.D., Group Head. E-mail: gerald.hagemann@dlr.de. Member AIAA.

Introduction

A PROMISING altitude-adaptive nozzle concept, first proposed by Foster and Cowles[1] as early as 1949, which has recently gained a growing interest in Europe and the U.S., is the dual-bell nozzle.[2,3] This nozzle concept offers an altitude adaptation, achieved only by a nozzle wall inflection. In low altitudes, controlled and symmetrical flow separation occurs at this wall inflection (see Fig. 1a), which results in a smaller effective area ratio without generating dangerous side loads. In higher altitudes the nozzle flow is attached to the wall until the exit plane and the full area ratio is used (see Fig. 1b). Because of the higher area ratio, an increase in performance is achieved.

Until the present time, the only publicly published experiments were performed by Horn and Fisher.[2] Their cold-flow subscale nozzle tests proved the altitude adaptive capability of this nozzle concept, but also showed that additional losses in performance are induced in dual-bell nozzles. Figure 2 illustrates the typical performance of a dual-bell nozzle as a function of flight altitude in comparison with two baseline bell-type nozzles with the area ratios of the dual-bell base nozzle and of the dual-bell nozzle extension, respectively. At sea-level operation, the pressure within the separated flow region of the dual-bell nozzle extension is slightly below the ambient pressure, inducing a thrust loss, the aspiration drag. In addition, the flow transition from the sea-level mode to the altitude mode occurs before the optimum crossover point, which leads to a thrust loss compared with an ideal switchover. The nonoptimum contour of the full-flowing dual-bell nozzle in the altitude mode results in further losses. Despite these additional losses, the dual-bell nozzle still provides a significant net impulse gain over the entire trajectory compared with both baseline nozzles, as shown by trajectory analyses published in Ref. 3.

First numerical simulations of dual-bell nozzles were published by Goel and Jensen[4] who basically presented a recalculation of the previously mentioned cold-gas subscale experiments.

In this paper, numerical results of full-scale nozzles for a future launcher are presented. The dependence of additional losses induced in dual-bell nozzles as a function of nozzle design parameters is systematically investigated, and performance characteristics are compared with a conventional reference bell nozzle.

Design Aspects of Dual-Bell Nozzles

Inner Contour, Base Nozzle

The inner contour part of a dual-bell nozzle, also named the base nozzle, is in general designed as a Rao-type bell nozzle

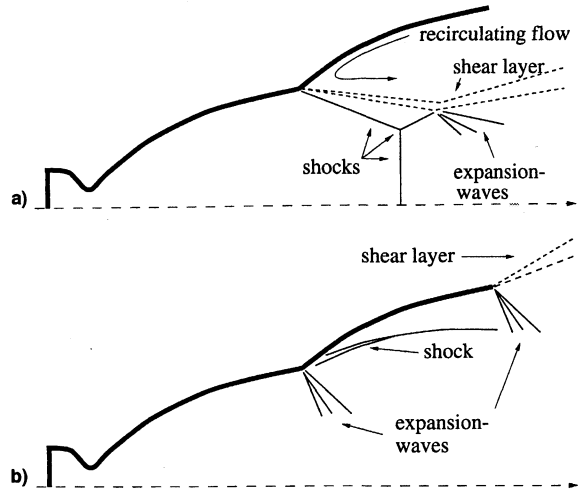

Fig. 1 Different flow regimes in dual-bell nozzles: a) sea-level mode with flow separation at the wall inflection point and b) altitude mode with a full-flowing nozzle.

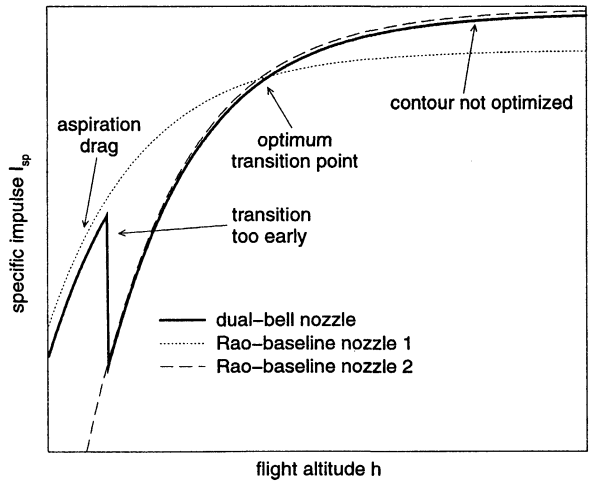

Fig. 2 Performance of a dual-bell and two baseline nozzles as function of flight altitude (baseline nozzle 1: same area ratio as dual-bell base nozzle; baseline nozzle 2: same area ratio as nozzle extension).

for maximum performance. These types of nozzles, which are commonly used in the space industry, have an approximate length of 70–85% of a 15-deg cone nozzle with the same exit area ratio. However, this rough design approach is not applicable for the estimation of the base nozzle length of dual-bell nozzles because the choice of the base nozzle length also influences vacuum performance of the full-flowing dual-bell nozzle, as will be shown later in this paper. Thus, a tradeoff between nozzle weight and performance for both operation modes must be performed to find the best length ratios of base nozzle and nozzle extension.

Wall Inflection and Nozzle Extension

The wall pressure profile of a dual-bell nozzle within the base nozzle is equivalent to the one of conventional bell nozzles. At the wall inflection, a Prandtl–Meyer expansion accelerates the flow. To ensure controlled flow separation at the wall inflection within a certain range of ambient pressures, the required wall pressure value behind the wall inflection can be estimated with commonly used separation criteria, such as Summerfield et al.[5] or Schmucker.[6] The corresponding wall inflection angle, γ, can then be calculated using the well-known Prandtl–Meyer equations.

In a graph showing wall pressure vs nozzle length, as shown in Fig. 3, a separation criterion can be introduced as a line or

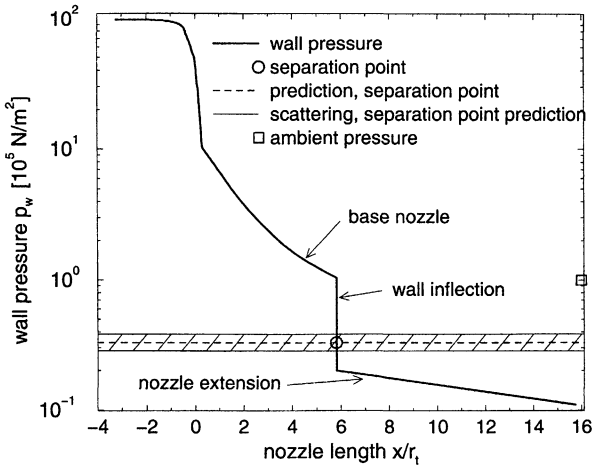

Fig. 3 Wall pressure profile for expansion into vacuum; dual-bell nozzle extension with favorable pressure gradient. Application of separation criterion at 1 bar ambient pressure, flow separation at $x/r_t = 5.9$.

bar. The nozzle part with wall pressure values above the line is full flowing, whereas the region with pressure values lower is fully separated. During the sea level mode, the pressure limits given by the line of the separation criterion must therefore intersect the wall pressure profile within the pressure drop at the wall inflection, as shown in Fig. 3. This controlled flow separation at the wall inflection prevents the generation of dangerous side loads commonly observed in conventional overexpanded nozzles.

Ambient pressure continuously decreases during the ascent of the rocket. In the wall pressure graph, this is linked to a movement of the separation line toward lower pressures. At a certain ambient pressure, the bar of the separation criterion intersects the wall pressure profile in the nozzle extension. Different designs of this extension, producing a favorable, zero, or even an adverse wall pressure gradient, will lead to different flow behavior:

1) Nozzle extension with a favorable wall pressure gradient: This nozzle extension leads to an uncontrolled flow separation within the nozzle extension, as can be observed in conventional conical or bell-shaped nozzles.

2) Nozzle extension with zero wall pressure gradient (constant pressure extension): Within a nozzle extension producing a constant pressure profile, the horizontal bar of the flow separation criterion reaches all points of the nozzle wall at the same time. This might lead, at least theoretically, to a quick change from sea level mode to altitude mode.

3) Nozzle extension with adverse wall pressure gradient (overturned extension): The separation criterion intersects the wall pressure profile of nozzle extensions with positive pressure gradients first in the exit plane of the nozzle, but the full flowing of the nozzle extension first occurs at ambient pressures, where the bar reaches the wall inflection. Therefore, this type of nozzle extension also might lead, at least theoretically, to a quick change from a sea-level mode to an altitude mode. However, former experiments with conventional nozzles featuring an adverse pressure gradient revealed significant side-load problems.[6]

These considerations are confirmed by the experimental results of Horn and Fisher.[2] They observed a sudden movement of the separation point from the wall inflection to the nozzle exit only for model nozzles with constant pressure or overturned extensions. All other nozzle extensions experienced uncontrolled flow separation within the extension at intermediate ambient pressures.

The exact prediction of the flow separation point has not yet been fully solved and is the subject of ongoing research. Taking into account a certain scattering of the separation point has

a significant impact on the nozzle extension design. (This scattering converts the separation line into a separation bar of finite thickness.) The scattering is characterized by a lower and upper relative deviation, $\delta_{\text{rel},l}$ and $\delta_{\text{rel},u}$, respectively. The definition of relative deviations and the knowledge of minimum and maximum wall pressure values of the full-flowing nozzle extension allows one to define a critical wall pressure interval, $\Delta p_{w,\text{tr}}$, where unpredictable flow behavior might occur within the extension (see Fig. 4 for a favorable pressure gradient extension). For a constant pressure extension, as shown in Fig. 5, $p_{w,\min} = p_{w,\max} = p_w$ is valid, whereas for overturned extensions both pressure values must be replaced by the minimum pressure value directly behind the wall inflection.

This critical pressure interval, $\Delta p_{w,\text{tr}}$, can be translated into a critical ambient pressure interval, $\Delta p_{a,\text{tr}}$, by using the separation criterion of Schmucker,[6] which links the critical wall pressure ratio, $p_{w,\text{sep}}/p_a$, at the separation point to the inviscid flow Mach number, M_w, near the separation point. A transitional phase can now be defined, during which separation might occur rather arbitrarily within the extension. It is defined by the time interval during the launcher ascent, where the bar of the separation criterion covers parts of or the complete nozzle extension (Fig. 4). Assuming a simple isothermal model for the lower atmosphere, the duration of this phase results in (see Ref. 7 for further details)

$$T_{\text{tr}} = -\frac{\Delta p_{a,\text{tr}}}{\frac{\partial p_a}{\partial t}}$$

$$= \left\{ \frac{p_{w,\max}(1+\delta_{\text{rel},u})}{[1.88 \times M_{w(p_{w,\max})} - 1]^{-0.64}} - \frac{p_{w,\min}(1-\delta_{\text{rel},l})}{[1.88 \times M_{w(p_{w,\min})} - 1]^{-0.64}} \right\}$$

$$\times \frac{RT_{a,\text{sl}}}{p_{a,\text{sl}} g \times e^{-(g/RT_{a,\text{sl}})h} \times v(h)} \tag{1}$$

The interpretation of Eq. (1) explains why in real-flight hardware the duration of the transitional phase can be significantly longer compared with subscale experiments:

1) Because of limited running times in experiments, the pressure ratio p_c/p_a is often varied faster than is the case during the ascent of real launchers. The fact, that Horn and Fisher[2] did not observe any uncontrolled flow separation within the constant pressure extension might have been because they rapidly increased the pressure ratio of chamber pressure to ambient pressure, p_c/p_a, so that there was almost no significant transitional phase.

2) Any kind of instability in the propulsion system, which causes a fluctuation or oscillation of the chamber pressure,

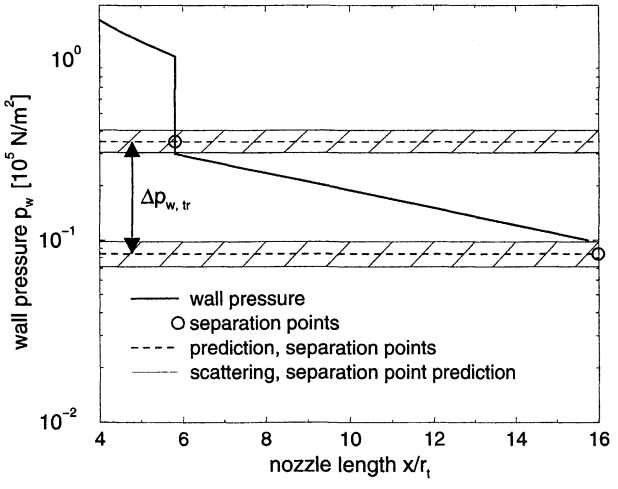

Fig. 4 Critical wall pressure interval.

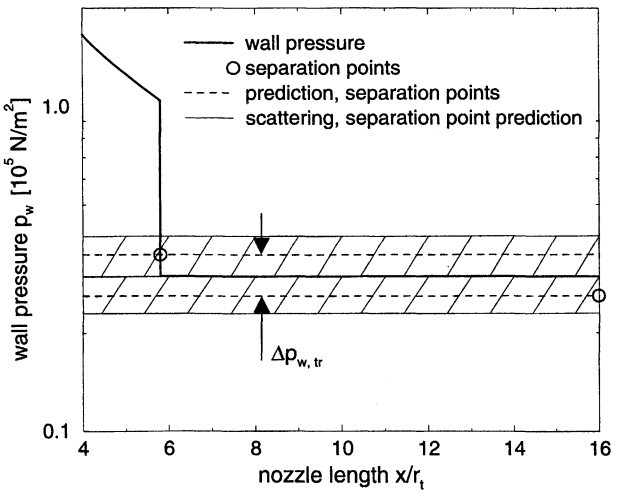

Fig. 5 Critical wall pressure interval.

leads to a broader scattering of the separation point and, thus, to an increase of $\Delta p_{a,\text{tr}}$ and T_{tr}.

3) Hardware vibrations caused by acoustics, the rotation of compressors, turbines, etc., and interferences with ambient flow can influence the flow within the thin-shell nozzles, and might also lead to a stronger scattering of the separation point and, thus, to an increase of $\Delta p_{a,\text{tr}}$ and T_{tr}.

4) The nozzle models used in subscale tests often have a smooth, polished surface, in contrast to the relatively rough surfaces of real-flight hardware. Higher turbulence intensity might occur in real nozzles, which also influences the flow separation.

5) The Reynolds analogy is often disregarded in most subscale experiments, although recirculation depends on the Reynolds number. The extrapolation of these subscale experiments to realistic scales therefore remains uncertain. This is also the case for the experiments of Horn and Fisher.[2] Additionally, the Reynolds number in their experiment was not constant because the chamber pressure was varied during the tests to achieve different pressure ratios.

As an example, the duration of the transitional phase, T_{tr}, is estimated for the FSS-1 launcher, described in more detail in Ref. 3. Its potential engines have dual-bell nozzles with a constant pressure extension and a wall pressure level in the extension of $p_w = 0.15$ bar. In this case, the change in flow behavior from separated flow to the full flowing occurs at an ambient pressure level of ~0.55 bar, which corresponds to an altitude of 5400 m. A typical vertical velocity component at this altitude of existing launchers is $\sim v(h) = 300$ m/s. The comparison of the Schmucker criterion with available experimental data results in a deviation of experimental and theoretical data of $\delta_{\text{rel},u} = \delta_{\text{rel},l} \approx 8\%$, which finally results in a duration of the transitional phase, according to Eq. (1), of $T_{\text{tr}} \approx 5$ s for a constant pressure extension. A nozzle extension that produces a favorable pressure gradient, e.g., a nozzle extension for maximum specific impulse, in which a wall pressure drop of 0.1 bar occurs between wall inflection and nozzle exit, has a longer duration, which results in $T_{\text{tr}} \approx 25$ s.

Within the contour design process of a dual-bell nozzle extension, the following remarks must be taken into account:

1) The constant pressure extension will induce maximum side forces during the transitional phase, wherein the nozzle operation changes from the sea level mode with separated flow at the wall inflection to the altitude mode with the full-flowing nozzle. However, the duration of this transitional phase is short. It may even be so short that the side loads do not occur, as indicated in the experiments performed by Horn and Fisher.[2]

2) Side loads will be induced in extensions with a favorable pressure gradient because the duration of the transitional phase

is significantly longer compared with the nozzle extension with a constant pressure extension.

Further experiments with a time-accurate simulation of realistic flight conditions and, thus, of the critical time interval, will give valuable information on the side-load behavior.

For the parametrical numerical simulations, different nozzle extensions were designed, including constant-pressure, overturned, and conical extensions.

Parametrical Variation of Dual-Bell Nozzle Design Parameters

Based on results of a combined launcher and trajectory optimization published in Ref. 3, numerical simulations of dual-bell nozzles were performed. A conventional, Rao-type bell nozzle was used as the reference nozzle. The geometrical design data and chamber stagnation conditions of the dual-bell and the reference bell nozzle are summarized next: r_t = 145 mm, ε_B = 48, ε_E = 115, ε = 115, propellants = H_2/O_2, o/f = 6.6, p_c = 150 bar, and T_c = 3680 K. Numerical simulations were performed for the reference bell nozzle with a finite volume scheme,[8] and for verification also with a finite difference scheme[9] and TDK.[10] The additional numerical simulations of the dual-bell nozzles were performed only with the finite volume scheme.[8] With regard to the numerical simulations of dual-bell nozzles, this code has been validated with experimental data of overexpanding conventional nozzles, and with experimental data of the Horn and Fisher experiment (see Ref. 8). Further test-case simulations were performed on rather simple flow conditions, where analytical solutions exist.

The numerical analyses were performed with the assumption of local chemical equilibrium in the nozzle. Turbulence was simulated with either an algebraic turbulence model or a two-equation k-ε model. The TDK analysis was performed with the assumptions of local chemical equilibrium and finite rate chemistry, respectively.

Vacuum Performance

The performance prediction with TDK and the calculated nozzle efficiencies of the reference bell nozzle for the different loss origins, including chemical nonequilibrium, friction, and multidimensional effects are summarized next: specific impulse, ODE-analysis = 4625 m/s; kinetic efficiency = 0.999; friction efficiency = 0.993; divergence efficiency = 0.995; nozzle efficiency = 0.987; and resulting specific impulse = 4568 m/s. This identification of the individual loss effects will be helpful for an understanding of the different loss origins in dual-bell nozzles. The performance values of the reference bell nozzle will be used in the comparison of this nozzle with the dual-bell nozzles, to obtain some information about the additional loss in altitude performance caused by the wall inflection. The influence of different contour parameters of the nozzle, such as the ratio of base nozzle length to total length of nozzle; the angle at the wall inflection, γ, and the exit angle of the nozzle extension, β_E; and the type of the nozzle contour downstream of the wall inflection (parabolas and smoothed parabolas or freejet contours for constant pressure extensions) on the flowfield and on the integral performance data were systematically investigated. Corresponding angle definitions are shown in Fig. 6. The overall lengths of all simulated dual-bell nozzles are the same as for the reference nozzle. Four different base nozzles with a 55, 65, 75, and 85% length of a 15-deg cone nozzle, respectively, each with a Rao-type contour for maximum performance, were chosen. In the following, these base nozzles are numbered 0, 1, 2 and 3, respectively.

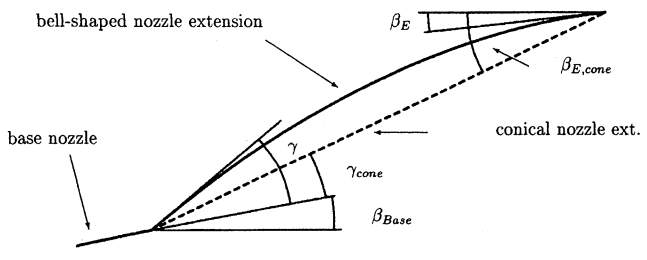

Fig. 6 Contour angles of nozzle extension.

As had been previously expected, the numerical simulations of the isolated base nozzles showed that the longer base nozzles have a better vacuum performance, because of smaller divergence and profile losses.

Figure 7 summarizes all vacuum performance data of the simulated dual-bell nozzles. It shows the ratio of vacuum performance data of the dual-bell nozzle and the reference bell nozzle as a function of all dual-bell nozzle design parameters and, thus, illustrates the loss in performance caused by the nonoptimum contour of dual-bell nozzles. The first group of curves in Fig. 7, marked with index 0, shows the ratio of specific impulse of the dual-bell nozzles based on base nozzle no. 0, the other groups of curves marked with 1, 2, and 3 show corresponding values of the other dual-bell nozzle families based on base nozzles 1, 2, and 3.

The curves reveal a strong dependence of the performance data on the length ratio of the base nozzle and the nozzle extension. The dual-bell nozzle with the longest base, nozzle 3, had the poorest vacuum performance data, whereas the dual-bell nozzle with the shortest base, nozzle 0, had the highest performance data because of high and low divergence losses, respectively. This result is in contrast to the performance of the isolated base nozzles, indicating the necessity of the tradeoff study for the length ratios.

The vertical, dotted lines at the right end of all curves correspond to the nozzle exit angle, β_E, of a conical nozzle extension, $\beta_E = \beta_{\text{Base}} + \gamma_{\text{cone}}$, which represents a limit for realistic dual-bell nozzle extensions. Higher nozzle exit angles were not the subject of this investigation because the contour then approaches a trumpet-like form. The thicker lines emphasize the specific impulses of the dual-bell nozzles with contour turn angles that ensure flowfield transition at the ambient pressure levels, which were specified by the combined launcher and trajectory optimization published in Ref. 3.

At higher exit angles, β_E, the influence of the contour turn angle at the wall inflection γ diminishes because shortly behind the wall inflection the parabolic nozzle contours approach the conical contour. The same tendency is observed for the variation of the exit angles, β_E, at prescribed contour turn angles, γ, close to the conical one, γ_{cone}.

The overall magnitude of the performance losses caused by the improper contour is in the range of the divergence loss origin of the reference nozzle, which is a surprisingly low value.

Sea Level Performance

Numerical simulations were performed for the dual-bell nozzle with base nozzle 2 and with the nozzle extension for maximum performance at different ambient pressures, p_a = 1 bar, 0.8 bar, ($p_{a,\text{tr}}$ + 20%), and 0.5 bar ($p_{a,\text{tr}}$ − 20%). The ambient gas was assumed to be air, with a temperature of T_a = 300 K and an isentropic coefficient of κ = 1.4.

The separation of the flow at the wall inflection was observed at the ambient pressures of p_a = 1 and 0.8 bar ($p_{a,\text{tr}}$ + 20%). Full flowing is predicted with the numerical scheme at an ambient pressure of p_a = 0.5 bar ($p_{a,\text{tr}}$ − 20%). These results are in good agreement with the theoretical prediction of the flowfield development using a separation criterion. The flowfield development at different ambient pressures indicates that the design of the dual-bell nozzle contour with a commonly used separation criterion leads to reasonable results within a certain tolerance.

The pressure within the separated flow region in the nozzle extension for ambient pressures of p_a = 1 and 0.8 bar results in $p_{w,E} \approx (1 - \Pi) \times p_a = 0.9 \times p_a$. ($\Pi$ is the relative difference between the ambient pressure and the wall pressure in the re-

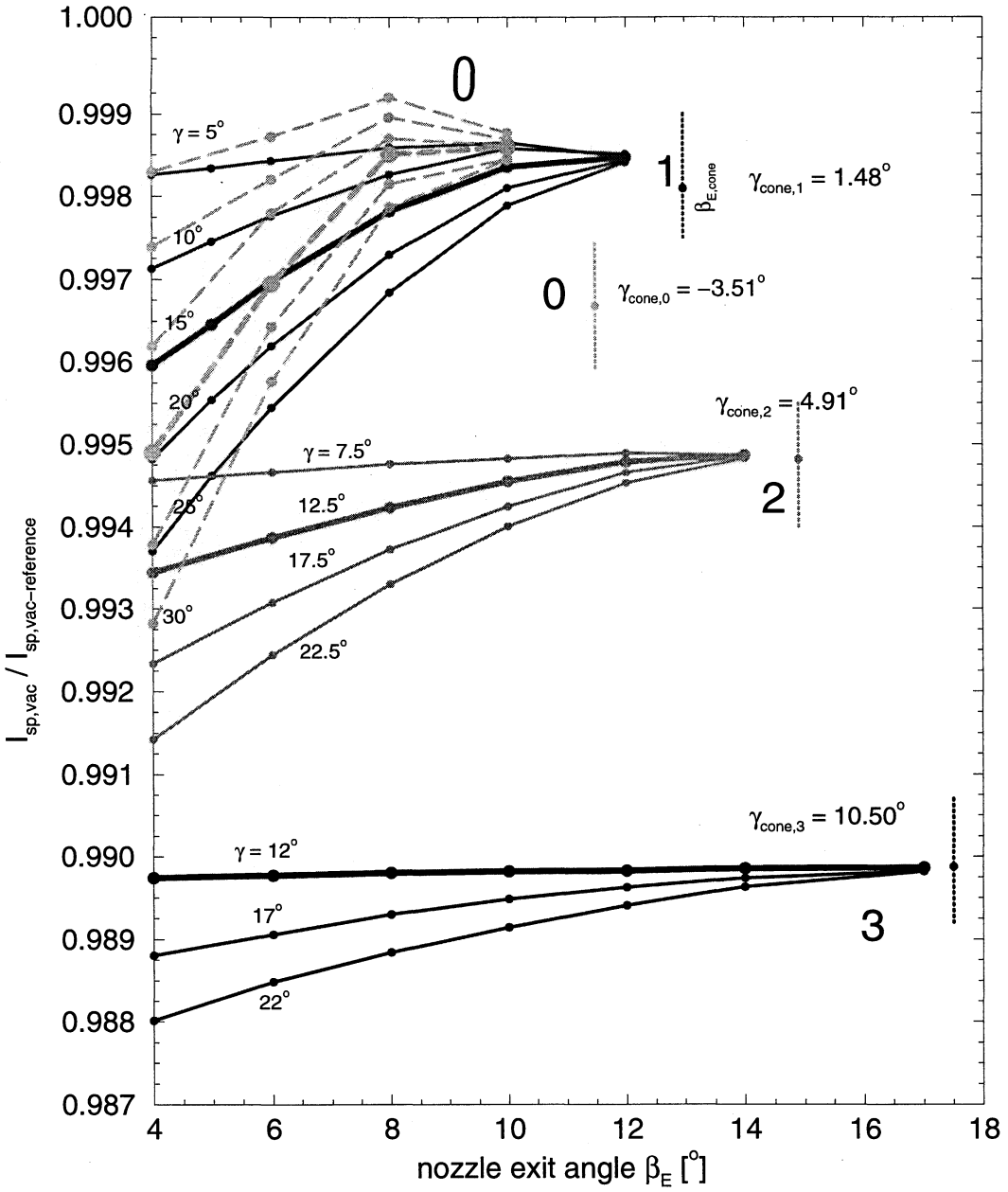

Fig. 7 Specific vacuum impulses of all simulated dual-bell nozzles with parabolic extensions.

circulation zone behind the wall inflection, with Π = 10% according to Ref. 7.) This is again in agreement with experimental results of Horn and Fisher.[2]

Further numerical simulations showed that the dual-bell nozzles with the longest base, no. 3, have the highest sea-level performance because of the best-performing base nozzle with the lowest divergence and profile losses.

Because the thrust loss caused by the aspiration drag during sea-level operation is approximately the same for all dual-bell nozzles, their sea-level performance is directly connected to the performance of the isolated base nozzles. The numerical simulations revealed an additional loss caused by this aspiration drag of ~3% at takeoff, which decreases linearly with the ambient pressure.

Flow Transition Control on Engine System Level

As pointed out in the Introduction, the transition from the sea-level mode to the altitude mode is crucial for the feasibility of the dual-bell concept. It was mentioned earlier that even with a constant pressure extension, it cannot be guaranteed that there are no side forces during the transition. Thus, there can be two ways to handle this critical phase:

1) The structure of the nozzle could be designed in a way that it is able to bear such forces without damage. In this case, the flight control would also have to be adapted to the lateral forces.

2) The duration of the transition, T_{tr}, could be further reduced until a sufficiently short time is reached where damage to the nozzle does not occur.

Because the first of these two alternatives is connected with a much higher weight of the nozzle, the second suggestion is chosen here. The idea consists of continuously lowering the chamber pressure and, thus, delaying the transition from the sea-level mode to the altitude mode. Later, p_c is suddenly raised back to its original value. During this fast rise of the chamber pressure, a sudden and side-load-free transition should be reached.

The throttling of the chamber pressure begins shortly before the transition from the sea-level mode to the altitude mode would take place, if p_c was kept constant. The chamber pres-

sure is lowered in a way that the ratio p_c/p_a remains constant. This ensures that both the ratio p_w/p_a and the inviscid flow Mach number near the wall, M_w, which are the decisive parameters for flow separation, remain constant and that there will be no transition. The chamber pressure is continuously lowered until the specific impulse in the altitude mode with full chamber pressure exceeds the specific impulse that is reached in the sea-level mode with a reduced chamber pressure.

The specific impulse for a dual-bell nozzle operating in the sea-level mode is computed as follows:

$$I_{sp} = w_{e,B} + \frac{(p_{e,B} - p_a)A_B}{\dot{m}} - \underbrace{\frac{\Pi p_a(A_E - A_B)}{\dot{m}}}_{\text{asp.drag}} \tag{2}$$

$w_{e,B}$ is the averaged velocity in the exit plane of the base nozzle; $p_{e,B}$ is the pressure in this plane, and A_B and A_E are the exit areas of the base nozzle and the nozzle extension, respectively. The mass flow for the reduced chamber pressure finally results in[7]

$$\dot{m} = \underbrace{\dot{m}_{ref}\frac{\sqrt{T_{c,ref}}}{p_{c,ref}}}_{\text{const.}} \times \frac{p_c}{\sqrt{T_c}} \tag{3}$$

with the "reference condition" before the chamber pressure is lowered. The specific impulse for the reduced chamber pressure follows as

$$I_{sp} = w_{e,B} + \sqrt{T_c} \times \overbrace{\frac{p_a}{p_c}\frac{p_{c,ref}}{\dot{m}_{ref}\sqrt{T_{c,ref}}}}^{\text{const.}} \times \underbrace{\left[\left(\frac{p_{e,B}}{p_a} - 1\right)A_B - \Pi(A_E - A_B)\right]}_{\text{const.}} \tag{4}$$

where only $w_{e,B}$ and $\sqrt{T_c}$ change as the chamber pressure is lowered. Typical engine throttling is reached by mixture ratio reduction, causing T_c to decrease. Because $w_{e,B}$ depends linearly on $\sqrt{T_c}$, and is barely affected by other parameters such as the thickness of the boundary layer or kinetic efficiency, I_{sp} will decrease linearly with $\sqrt{T_c}$.

For the considered launcher FSS-1 (Ref. 3), the nominal chamber pressure p_c = 150 bar should be lowered to a value of p_c = 116 bar to achieve an optimal I_{sp} profile. To obtain more information about the value of I_{sp}, further information about T_c as a function of the chamber pressure p_c is required, which is given by transient engine system analyses performed for the behavior of the Vulcain engine, taking into account two-phase flows in pipelines as well as inertia of turbines and pumps. The following dependence is derived:

$$\Delta T_c/T_c \approx 0.4 \times (\Delta p_c/p_c) \tag{5}$$

If this relation is assumed to be valid for the FSS-1 vehicle, mass flow, thrust, and specific impulse during the lowering of the chamber pressure can be predicted. As a result, I_{sp} decreases by ≈5%, and the thrust is diminished to about three-fourths of its original value, while p_c is lowered. However, this means that a minor performance gain is achieved by the suggested chamber pressure variation compared with an identical engine with a constant chamber pressure (Fig. 8).

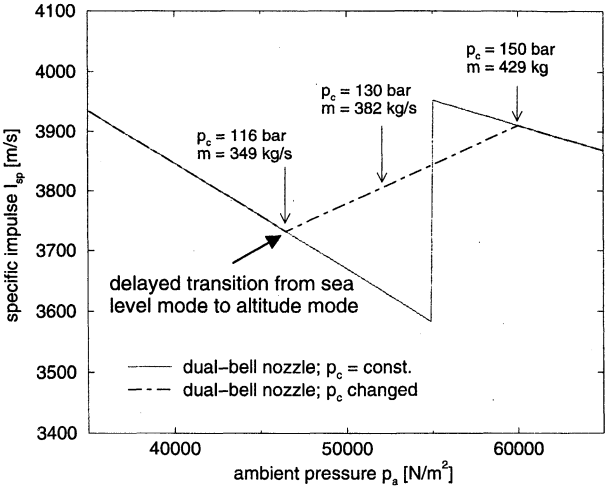

Fig. 8 Specific impulse, chamber pressure, and mass flow as a function of ambient pressure.

To estimate the duration of the transitional phase with uncontrolled separation in the nozzle extension in a typical case, a constant pressure extension is considered, and Eq. (1) reduces to

$$T_{tr} = -\frac{\Delta(p_a/p_c)_{tr}}{\frac{\partial(p_a/p_c)}{\partial t}} = \frac{\overline{p_w}(\delta_{rel,u} + \delta_{rel,o}) \times (1.88M_w - 1)^{0.64}}{\underbrace{\frac{p_{a,sl}g}{RT_{a,sl}}e^{-(g/RT_{a,sl})h}v(h)}_{\text{ascent}} + \underbrace{\frac{p_a}{\overline{p_c}}\frac{\partial p_c}{\partial t}}_{\substack{\text{chamber}\\ \text{press. var.}}}} \tag{6}$$

where $\overline{p_w}$ and $\overline{p_c}$ are averaged values during the chamber pressure rise. The numerator of this equation consists of two terms; the first one considers the decreasing ambient pressure because of the launcher ascent, whereas the second one describes the changes in chamber pressure.

Again, the FSS-1 launcher is used as an example to get an insight into the duration of the transition from the sea-level mode to the altitude mode, as was done earlier without chamber pressure variation. Apart from the values for the ascent term [altitude h = 6800 m, $v(h)$ = 500 m/s], only $\partial p_c/\partial t$ is unknown. The transient simulation of the Vulcain engine revealed that 0.5 s are required for a pressure jump from 80 to 112 bar, so that $\partial p_c/\partial t \approx$ 64 bar/s for the Vulcain engine. If FSS-1 is assumed to show a similar behavior, and with p_a = 0.46 bar, $\overline{p_w}$ = 0.13 bar, and $\overline{p_c}$ = 133 bar, the duration will be $T_{tr} < 0.4$ s. As compared with the ≈5 s transition discussed previously, the chamber pressure variation shortens transition by more than one order of magnitude. The only way to significantly further shorten T_{tr} would be to increase $\partial p_c/\partial t$ because it is the only really independent term in Eq. (6).

It is concluded that a variation of the chamber pressure during the ascent of the launcher enhances the performance and shortens the dangerous transition from the sea-level mode to the altitude mode.

Conclusions

A critical assessment of dual-bell nozzles was given in this paper. Different design aspects for the wall inflection and nozzle extension were discussed, with special regard to the dependence of the transition behavior from sea level to altitude operation on the type of nozzle extension. A sudden transition from sea level to altitude operation is desirable, to avoid uncontrolled flow separation and side loads. Analytical and experimental results lead to the conclusion that two different types of nozzle extensions, the constant pressure extension and

the overturned extension, might offer the sudden flow transition. However, a critical analysis of transition behavior using a commonly used flow-separation criterion (including scattering) and a launcher trajectory showed that for a rather long period of several seconds, an uncontrolled flow separation within the nozzle extension may occur. This flow situation would then induce an extreme side-load force during the transitional phase of the constant pressure extension.

Flow and performance behavior of dual-bell nozzles were studied, with parametric variations of contour design parameters. As a result, the vacuum performance parameters show minor degradations because of the imperfect contour, compared with an optimized bell nozzle with the same total length and exit area ratio. The losses caused by the wall inflection have the same order of magnitude as the divergence loss of the reference bell nozzle.

The simulations of the sea-level operation revealed additional performance losses (less than 3%) for these dual-bell nozzles, resulting from a wall pressure level within the nozzle extension that is slightly below the ambient pressure. This additional performance loss depends linearly on the ambient pressure and, therefore, decreases during the ascent of the launcher. Furthermore, these simulations showed that the application of commonly used separation criteria, derived for conventional nozzles, give reasonable results when applied to dual-bell nozzles with wall inflection.

However, no further information was gained from these numerical simulations with regard to the transition from the sea-level mode to the altitude mode, which is crucial for the feasibility of the dual-bell concept. It has been shown analytically that the duration of flow separation in the nozzle extension can be shortened by approximately one order of magnitude by throttling the engine. In addition, the variation of the chamber pressure during the ascent of the launcher slightly enhances the performance during this critical flight period.

Acknowledgment

A part of this work was performed within the FESTIP-programme of the European Space Agency (ESA), published as ESA Contract 11.482/95/NL/FG. The authors gratefully acknowledge H. Immich (Dasa) and M. Caporicci (ESA) for financial support and permission for its release. The authors give special thanks to H.-D. Saßnick, who performed the transient engine analysis.

References

[1]Foster, C., and Cowles, F., "Experimental Study of Gas-Flow Separation in Overexpanded Exhaust Nozzles for Rocket Motors," Jet Propulsion Lab., California Inst. of Technology, Progress Rept. 4-103, Pasadena, CA, 1949.

[2]Horn, M., and Fisher, S., "Dual-Bell Altitude Compensating Nozzles," NASA-CR-194719, 1994.

[3]Immich, H., and Caporicci, M., "FESTIP Technology Developments in Liquid Rocket Propulsion for Reusable Launch Vehicles," AIAA Paper 97-3311, 1997.

[4]Goel, P., and Jensen, R., "Numerical Analysis of the Performance of Altitude Compensating Dual-Bell Nozzle Flows," *7th Annual Symposium*, Vol. II, NASA Marshall Space Flight Center, AL, 1995.

[5]Summerfield, M., Foster, C., and Swan, W., "Flow Separation in Overexpanded Supersonic Exhaust Nozzles," *Jet Propulsion*, Sept. 1954, pp. 319–321.

[6]Schmucker, R., "Flow Processes in Overexpanding Nozzles of Chemical Rocket Engines," Technical Univ. of Munich, Rept. TB-7, -10, -14, Munich, Germany 1973 (in German).

[7]Hagemann, G., Frey, M., and Manski, D., "A Critical Assessment of Dual-Bell Nozzles," AIAA Paper 97-3299, 1997.

[8]Hagemann, G., Krülle, G., and Hannemann, K., "Numerical Flowfield Analysis of the Next Generation Vulcain Nozzle," *Journal of Power and Propulsion*, Vol. 12, No. 4, 1996, pp. 655–661.

[9]Hagemann, G., Schley, C.-A., Odintsov, E., and Sobatchkine, A., "Nozzle Flowfield Analysis with Particular Regard to 3D-Plug-Cluster Configurations," AIAA Paper 96-2954, 1996.

[10]Nickerson, G., Dang, L., and Coats, D., Two Dimensional Reference Computer Program, NAS 9-12652, NASA Marshall Space Flight Center, AL, April 1973.